05M-507

A High Resolution Technique for Measuring Thru-Thickness Stresses in Sheet Metal

Thomas Gnaeupel-Herold
NIST Center for Neutron Research, University of Maryland

Tim Foecke, Mark Iadicola, Steve Banovic
National Institute of Standards and Technology, Metallurgy Division

ABSTRACT

In the Numisheet 2005 benchmark 3 four different automotive materials - AKDQ, HSLA 50, DP 600, and AA6022-T43 - were subjected to a channel draw process with different levels of draw bead penetrations, resulting in varying degrees of springback. Resulting specimen thicknesses were < 1 mm. The numerical prediction of the springback amplitudes was an important part of the benchmark; however, only limited experimental results were available to verify the residual stresses used to predict the springback. In this work, we present a high resolution X-ray diffraction technique that was used to determine the thru-thickness residual stresses responsible for springback. Using standard equipment, spatial resolutions down to 0.05 mm were achieved with data acquisition times of several hours or more, depending on the material. Specimen size limitations exist, and cross section surfaces need to be polished or electro-polished. Thus, the technique is particularly suited for residual stress determination on sheet metal in the thickness range > 0.5 mm where specimen dimensions can be as small as 25 mm to 50 mm without affecting the stress component of interest.

INTRODUCTION

The push to improve the accuracy of finite element predictions in sheet metal forming invites the comparison with experimental data that is intermediately related to the materials behavior as goal of the FEM modeling. An example is springback which is known for the considerable cost it causes in the tryout phase for forming tool development. Insufficient accuracy of springback prediction for a given tool geometry causes another round of refinement of the tool geometry until the final and desired shape is reached. Recent advances in finite element modeling together with enormous increases in computing power have enabled the application of this technology to daily production work. The results have been mixed, however, with good accuracy for some parts and insufficient accuracy for others. This is in no small part due to the complex nature of springback which is a scalar property originating from the equilibration of a bending moment induced by through-thickness residual stresses. The latter stem from plastic strains that are non-uniform though-thickness and generally in all directions of space. These strains are predicted based on the stress-strain properties of the material. It is obvious that improving the springback prediction is difficult without additional experimental data, and with so many parameters affecting the final outcome. The additional data can be obtained from the through-thickness residual stresses which are experimentally accessible and closely related to springback. Techniques for measuring the residual stress profiles non-destructively have been developed recently. However, due to the spatial resolution required (≈ 0.1 mm) there is a degree of experimental sophistication necessary including neutron diffraction and synchrotron x-ray diffraction [7,8] that has limited such measurements to a few selected samples. Improvements over these techniques are presented here using a very recently developed formalism that, using simple x-ray diffraction equipment, allows the determination of stress profiles on the length scale ≈ 1 mm with spatial resolutions of the order of 0.05 mm. This method was applied to small strips that were cut from the NUMISheet side wall of channel drawn panels in such a way to preserve the stresses of interest. Spatial resolutions in the x-ray measurements were nominally 0.05 mm which is sufficient to provide between 10 and 20 through-thickness stress values. This work presents results of such measurements on selected specimens of the Numisheet '05 Benchmark 3.

BENCHMARK AND SAMPLES

The details and the purpose of the benchmark, as well as materials property data, were presented in earlier publications [1,2,3,4], thus only an outline together is

presented here. The forming geometry is shown in Figure 1.

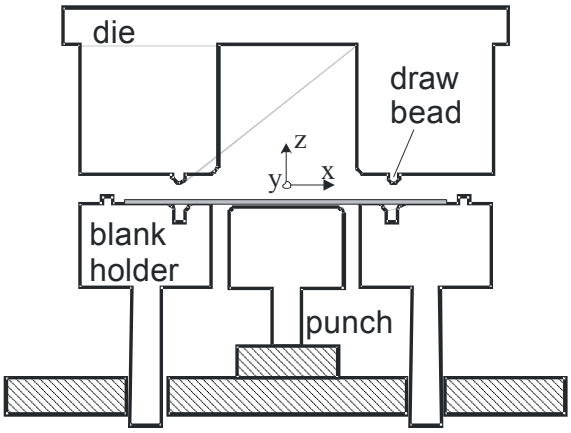

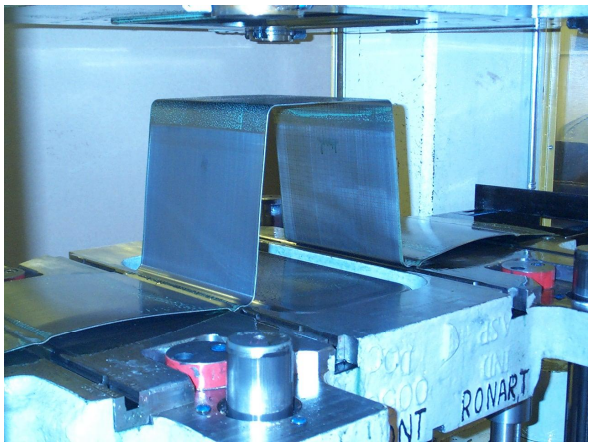

Figure 1. Setup of the channel draw process as presented in [3].

A number of steps were necessary to produce samples suitable for x-ray diffraction. The side panels were trimmed, and smaller specimens (x=25 mm, y=12 mm, $z \leq 1$ mm) were removed by means of electro-discharge machining. The specimens were cast in a block of epoxy and their cross section surfaces polished to remove all influence of the EDM cutting (total removal ≈ 1 mm). The final polishing step was a 0.05 μm SiC suspension intended to provide a surface undisturbed by mechanical damage other than the forming process. Figure 2 shows the steps involved.

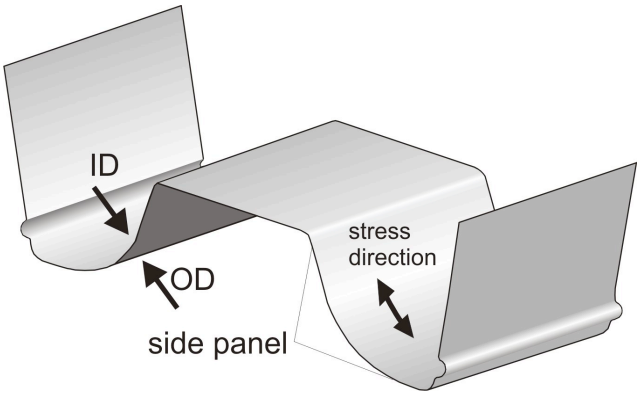

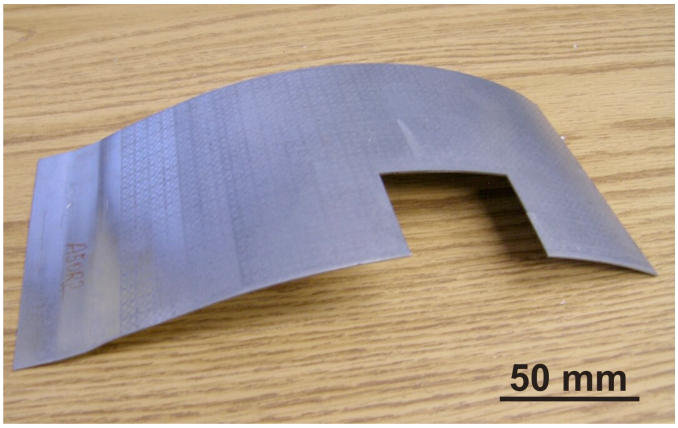

Figure 2. After the channel draw, the side panels (bottom) are cut from the u-channel, and smaller specimens are removed from the side panels.

The dimensions of the specimens were many multiples of the thickness, and it is a reasonable assumption that the stresses were left undisturbed by the removal procedure. The specimens used in the diffraction experiment are shown in Figure 3.

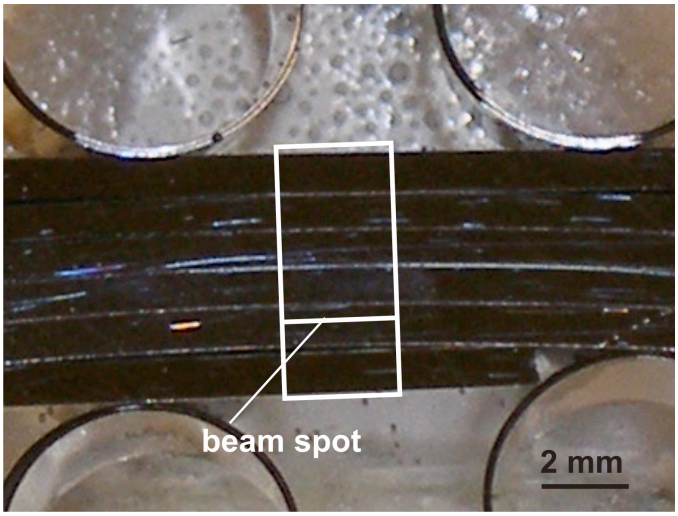

Figure 3. Example for the specimens used in the diffraction tests. The white rectangle indicates the measurement field with areas outside screened from diffraction by lead foil. The white line inside is an exaggerated depiction of the beam spot which is thinner in reality.

X-RAY MEASUREMENT PROCEDURE

X-ray stress evaluation is based on the measurement of changes of interplanar lattice spacings of atoms in crystalline materials through Bragg's equation

$$\lambda = 2d_{hkl}\sin\theta \qquad \textit{eq. 1}$$

λ is the x-ray wavelength, d_{hkl} is the lattice spacing for the plane defined by the Miller indices (hkl), and θ is the Bragg angle. As with any strain gage based stress measurement, strains have to measured in more than one direction, thus the need to rotate or tilt a specimen. Through-thickness stresses are not an obvious subject of an x-ray (surface limited) stress measurement. The choice for measuring such sub-surface stresses is usually to use a bulk-penetrating neutron or synchrotron x-ray technique as discussed in [4,7,8,11]. However, the same stresses are "visible" to surface limited x-ray techniques on the cross section surface, provided that strains on a sufficiently small area can be measured. Thus, the task is to measure the stresses in the x-direction (see Figure 1, Figure 2, top) on the polished cross sections shown in Figure 3. It is clear that in order to resolve the stress profile sufficiently an x-ray beam having a width in the z-direction < 0.1 mm has to be employed. The impact of the small beam on data collection time is a prolonged counting time (5-10 times longer). On the positive side it should be noted that x-ray equipment costs and availability put the technique presented here ahead of other methods.

The formalism used here differs in some crucial aspects from commonly used procedures for X-ray diffraction stress analysis [9,10]. It is common practice to use large primary beams that are, depending on the tilt mode, either circular with > 1 mm diameter (psi-mode) or rectangular beams with several millimeters of height and ≈ 1 mm horizontal width (omega-mode). In both tilt modes the beam spot increases in width or covers different portions of the specimen surface with increasing tilt angle. It is obvious that in these cases strains are measured and averaged over areas several millimeters across. Consequently, the beam spot on the specimen surface is between one and two orders of magnitude too big for through-thickness stress fields in sheet metal. The solution to the insufficient spatial resolution is to define, through slit systems, a x-ray beam that is narrow in one dimension but wide in the other dimension. The first requirement is derived directly from the desired spatial resolution (e.g. 0.05 mm for sheet metal with ≈ 1 mm thickness), and the second requirement is a concession to the data acquisition time which is inversely proportional to the size of the illuminated area.

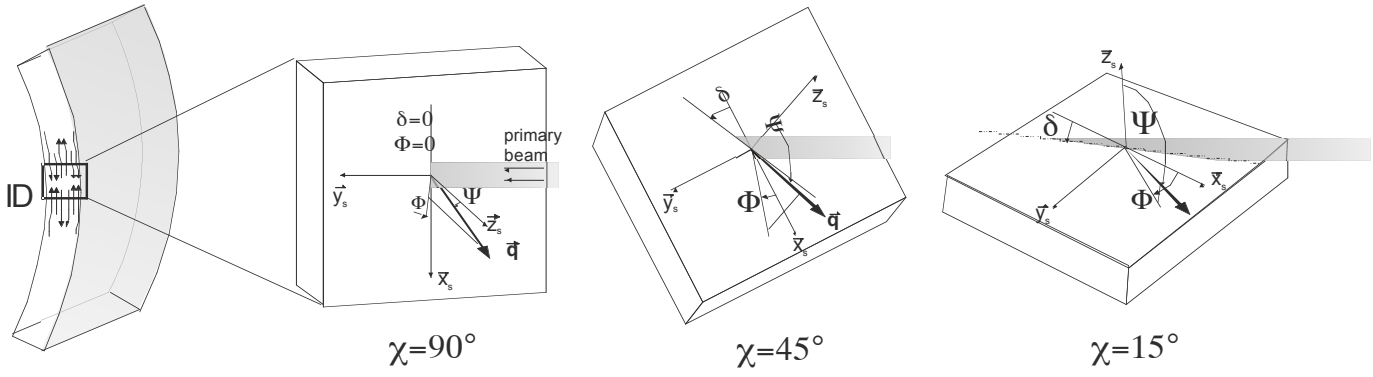

Figure 4. Measurement of a through-thickness stresses using a narrow beam. The reference frame used here adheres to the one usually used in x-ray diffraction with the z-axis perpendicular to the surface. Note that the reference frame of the forming ram has the z-direction parallel to the through-thickness direction. The vector $\vec{q}$ denotes the direction in which the strain is measured, and Φ, Ψ describe the orientation of $\vec{q}$ within the specimen's reference frame. The label 'ID' refers to the inner diameter.

The tilt mode used here makes use of the fact that the specimen can be orientated in such a way that a long, narrow, rectangular beam spot has the same orientation on the specimen surface at every azimuth and tilt angle, thus providing constant spatial resolution at all angles. The spatial resolution is optimal if the plane defined by the primary beam is perpendicular to the specimen surface. The implementation is described in Figure 4. Generally, a tilt or rotation of the specimen causes a rotation of the beam spot described by the angle δ. This rotation can be corrected for by rotating the specimen to -δ. An explicit expression for δ is given in [5]. Note that with increasing sample tilt the beam spot increases in length. The change in length can be undesirable for curved specimens because different depths are averaged over with increasing length of the beam spot. This is dealt with by using absorbing masks attached directly on the specimen surface. For spatial resolutions near the nominal 0.05 mm slit opening masks of 2.5 mm were used for the specimens investigated here. Stresses are considered constant over the length of the beam spot. It should be noted that for reasons both of optimal spatial resolution (narrowest beam spot) and optimal strain resolution (uncertainty of the d-spacing measured) the Bragg angle of the interplanar lattice spacing measured should be as large as possible, generally > 140 °. As a drawback, the choice of possible reflections (hkl) is very limited.

The rotational degrees of freedom necessary for orienting the specimen are found in Euler goniometers commonly used in x-ray diffraction as shown in *Figure 5*. The angle calculations for obtaining the azimuth angle Φ and the tilt angle Ψ from the Euler angles are given elsewhere [5]. The result of a measurement with a series of orientations (Φ,Ψ) yields lattice strains $\varepsilon(hkl,\Phi,\Psi)$ that relate to the residual stresses through [9]

$$\varepsilon_{\Phi\Psi} = \frac{d_{\Phi\Psi} - d_0}{d_0} = \tfrac{1}{2} s_2(hkl) \times \left[\begin{array}{l} (\sigma_{11}\cos^2\Phi + \sigma_{22}\sin^2\Phi + \sigma_{12}\sin 2\Phi)\sin^2\Psi + \\ (\sigma_{13}\cos\Phi + \sigma_{23}\sin\Phi)\sin 2\Psi + \sigma_{33}\cos^2\Psi \end{array} \right] + s_1(hkl)(\sigma_{11} + \sigma_{22} + \sigma_{33}) \quad \text{eq. 1}$$

$d_{\Phi\Psi}$ is the interplanar lattice spacing measured at the azimuth angle Φ and the tilt angle Ψ, d_0 is the unstressed spacing, $s_1(hkl)$ and $\tfrac{1}{2}s_2(hkl)$ are diffraction elastic constants, *hkl* denote the Miller indices of the reflection, and σ_{ij} are the stress tensor components. Eq. 1 is linearized and solved by a least squares method.

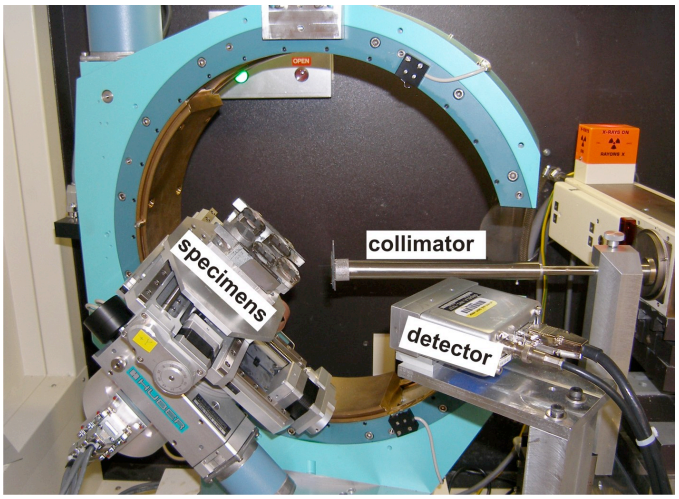

Figure 5. X-ray diffractometer in four circle configuration.

RESULTS

Results are presented for the minimum (25 %) and maximum (100 %) draw bead penetrations. Note that the stress distributions at 100 % draw bead penetrations have fewer data points due to the thickness reduction of ≈ 10 %. The thicknesses are listed in table 1. With the exception of AA6022-T4, the samples were zinc coated on both sides which is included in the thickness values.

Table 1. Sheet thickness in millimeters for samples with 25 % and 100 % draw bead penetrations. The accuracy is ± 0.01 mm.

DB penetration	AA6022-T4	AKDQ	HSLA 50	DP 600
25 %	0.98	0.94	0.79	1.00
100 %	0.85	0.81	0.72	0.90

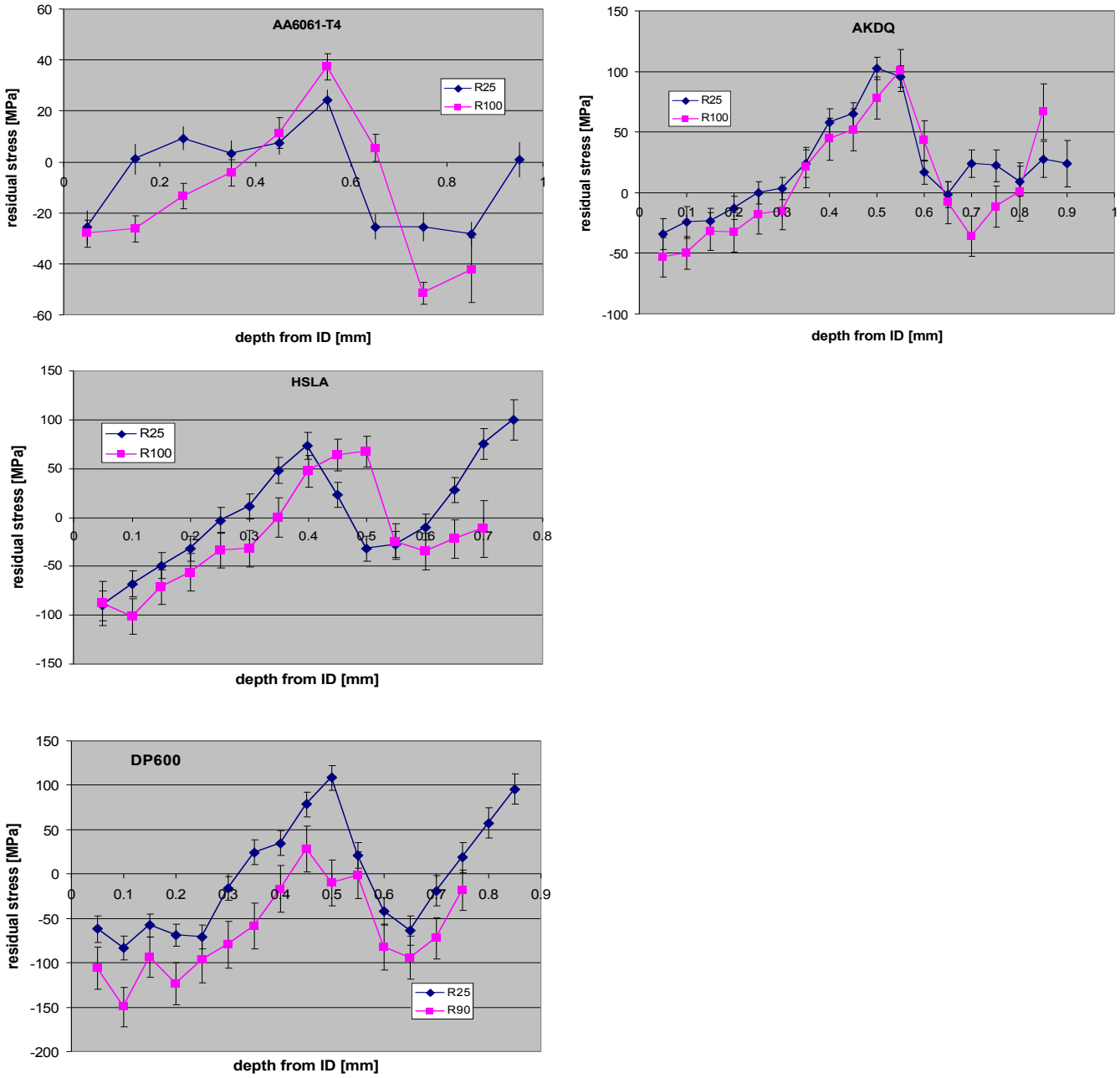

Figure 6. Through-thickness stresses in AA6022, AKDQ, HSLA 50 and DP600 (top to bottom) for 25 % and 100 % draw bead penetration.

The results shown in Figure 6 can be understood by considering the individual components of the plastic strains that comprise the forming process of the panels. By pulling the sheet through the draw bead the sheet undergoes the principal steps of bending, backbending, stretching, and, upon tool release, elastic springback. As residual stresses arise from non-uniform plastic strains, bending is the fundamental process responsible for through-thickness stresses as shown for HSLA in Figure 7.

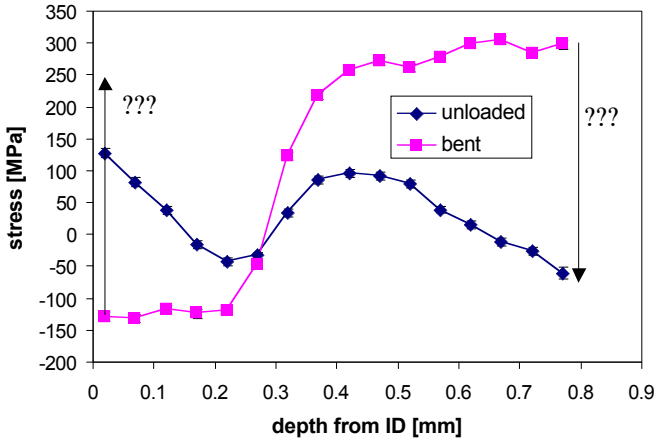

Figure 7. Through-thickness stresses for plastic bending of a HSLA 50 sheet with 0.80 mm thickness. The bending radius is r=46.8 mm, equivalent to ±0.86 % strain at the surfaces. In the unloaded state the radius is r=58.5 mm from which the stress difference $\Delta\sigma$ = ±370 MPa is calculated.

Deformation through stretching is uniform through thickness, thus the main effect of stretching on the residual stresses is a reduction of the stress maxima similar to a stress relief by plastic deformation. Bending-backbending sequences do not alter the principal shape but rather reverse the stresses with respect to the neutral plane. Figure 7 indicates also the presence of the Bauschinger effect through the visibly smaller compressive stress region in the bent state which can be explained by a decreased compressive yield strength.

INTERGRANULAR STRESSES

In order to obtain reliable results it is essential to consider intergranular stresses that arise in neighboring grains with different orientations and orientation dependent yield points. Diffraction measures changes in inter-planar atomic lattice spacings (hkl) on grains in specific orientations, and it is therefore subject to effects of this type of stress. Intergranular stresses can be subtracted my measuring a small coupon that is relieved from all long-range stresses (i.e. stresses that extend over the specimens dimensions), thus retaining only the intergranular stresses. However, this is not a viable approach because of the difficulties involved in producing samples small enough to achieve sufficient stress relief without introducing new stresses by the extraction procedure.
Here, two measures were taken to mitigate the effect of intergranular stresses: First, the stresses measured on the undeformed blank are subtracted, thus removing all preexisting intergranular stresses. This step also removes stress effects from the surface polishing, if any. Second, a portion of the intergranular stresses is introduced during forming, thus affecting different draw bead penetrations differently. The effects can be minimized by measuring stresses with different lattice planes (hkl) and subsequent averaging of the stresses. This is based on the equilibrium requirement that, in the absence of external forces, the sum of intergranular stresses for all grain orientations is zero. Two reflections ((310/(211)) were used for the steel samples, and three reflections were used for the AA6022 specimens ((311)/(331)/(420)). The use of more independent (hkl) is desirable especially for steel; however, with the available x-ray wavelengths only the two reflections (211) and (310) can be measured in the backscatter region ($2\theta > 140°$). Measurements should be performed in this region both for accuracy and for the low sensitivity to misalignment.

Stress balance and balance of bending moments are heuristic measures of the effect of intergranular stresses on the total stresses. Both are fulfilled satisfactorily for the lower strength, single phase materials AA6022, AKDQ and HSLA. DP600 differs with the two most likely reasons: first, the spread of intergranular stresses tends to increase with the yield stress, and second, intergranular stresses can be expected to increase with the difference between ultimate tensile strength (UTS) and yield strength. Both are the largest for DP600 with stress differentials between grains in the (310) and (211) orientation reaching 200 MPa (see Figure 8). Figure 8 also shows that the intergranular stresses are not uniform through the thickness as demonstrated by the fact that there is no simple offset/difference between the stresses measured using the (211) lattice planes and the (310) lattice planes.

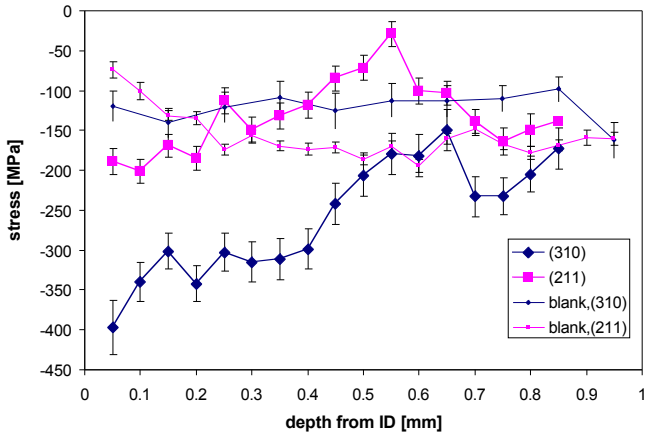

caption on same page?

Figure 8. Comparison of stresses measured on DP600 using different lattice planes in the undeformed state and 100 % draw bead penetration.

On the opposite end, the differential of intergranular stresses is smallest for AA6022 which has both the lowest yield stress and the lowest UTS. Stresses measured on three different lattice planes are shown in Figure 9.

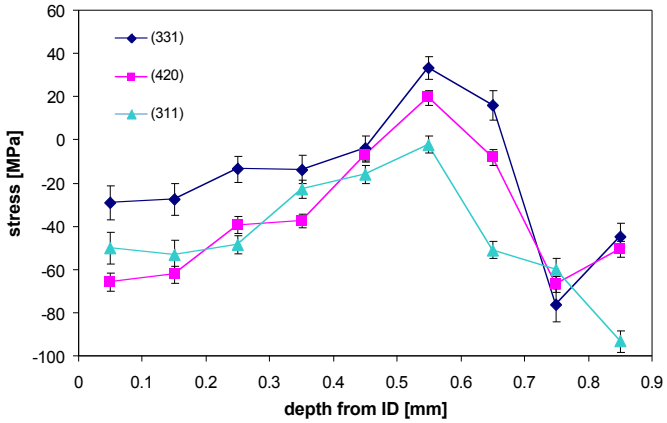

Figure 9. Stresses in the AA6022 panel with 100% penetration for three different lattice planes (hkl). The stresses in Figure 6, top were obtained by averaging the stresses shown here. ?

CONCLUSIONS

The through-thickness stresses on Numisheet 2005 benchmark 3 samples were measured for different materials and draw bead penetrations. The measurement procedure used offers new levels of resolution and detail, and it reveals that similar for all materials and draw bead penetrations the stress distributions can be explained by sequences of plastic bending. The results also demonstrate the presence of intergranular stresses which affect the stresses presented here to a minor degree.

REFERENCES

1. M. A. Iadicola, T. Foecke, and T. B. Stoughton (2005): “Experimental Procedures and Results for Benchmark 3: Stage 2 Forming Process”, Proceedings of Numisheet 2005, edited by J. Cao, M. F. Shi, T. B. Stoughton, C.-T. Wang, and L. Zhang, American Institute of Physics, CP778 Volume B, pp. 905-915.
2. D.E. Green, T.B. Stoughton, T. Gnaeupel-Herold, M.A. Iadicola, T.Foecke (2006): “Influence of drawbeads in deep drawing of plane-strain channel sections”, Proceedings of the International Deep Drawing Research Group 2006 Conference, June 19-21, 2006 - Porto, Portugal, edited by A.D. Santos and A. Barata da Rocha, pp. 559-566

3. M.C. Oliveira, A.J. Baptista, J.L. Alves, L.F. Menezes, D.E. Green, T. Gnaeupel-Herold, M.A. Iadicola, T. Foecke, T.B. Stoughton, Two Stage Forming: Experimental and FE Analysis, Proceedings of IDDRG, June 2006, Porto (Portugal), p. 279-286
4. Z. Cedric Xia, Craig E. Miller**,** Maurice Lou**,** Ming F. Shi, Alex A. Konieczny**,** X.M.Chen, Thomas Gnaeupel-Herold, A Benchmark Test for Springback: Experimental Procedures and Results of a Slit-Ring Test, SAE Trans.: J. Mater. Manufacturing **114**, 19 (2006).
5. T. Gnaupel-Herold, Formalism for the Determination of Intermediate Stress Gradients using X-ray Diffraction, submitted to Journal of Applied Crystallography
6. M.E. Hilley, SAE J784a: Residual Stress Measurement by X-Ray Diffraction, Society of Automotive Engineers, Warrendale, PA 1971
7. T. Gnaeupel-Herold, T.J. Foecke, H.J. Prask, R.J. Fields (2005), An Investigation of Springback Stresses in an AISI-1010 Deep Drawn Cup, Mat. Sci. Eng. **A399**, 26-32.
8. T. Gnaeupel-Herold, H. J. Prask, R.J. Fields, T.J. Foecke, Z.C. Xia and U. Lienert (2004) "A synchrotron study of residual stresses in a Al6022 deep drawn cup", *Materials Science and Engineering* **A366**, 104-113.
9. V. Hauk (ed.), *Structural and Residual Stress Analysis by Nondestructive Methods*, Elsevier Science B.V. Amsterdam (1997)
10. I. C. Noyan, J. B. Cohen, *Residual Stress Measurement by Diffraction and Interpretation*, Springer, New York (1987)
11. T.Gnaupel-Herold, T.J.Foecke, H.J.Prask, R.J. Fields, L.E. Levine, Z. Cedric Xia, U. Lienert, An Investigation of Springback Stresses in Deep Drawn Cups Using Diffraction Techniques, SAE Trans.: J. Mater. Manufacturing 114, 175 (2006).

CONTACT

For further information or questions and comments regarding this study, please contact Thomas Gnäupel-Herold at the NIST Center for Neutron Research at tg-h@nist.gov.